Surface roughening in shadowing growth and etching in 2+1 dimensions

Jason T. Drotar, Y.-P. Zhao, T.-M. Lu, and G.-C. Wang
Department of Physics, Applied Physics, and Astronomy, Rensselaer Polytechnic Institute, Troy, New York 12180-3590
(Received 18 October 1999)

Through numerical calculations and Monte Carlo simulations, we examine the roughening behavior of a shadowing model, with lateral growth, for $(2+1)$-dimensional systems. The results show that the roughening growth exponent $\beta=1$ for growth and $\beta=0$ for etching. For the Monte Carlo simulation of the growth model, tall columns are formed, and the correlation length obeys $\xi\propto(t-t_0)^{1/z}$, with $1/z=0.93\pm0.1$. For the Monte Carlo simulation of the etching model, we obtain $1/z=0$, and the height-height correlation function $H(r)$ is proportional to $\log(r)$ for $r\ll\xi$. The results are compared to previous computational studies of shadowing and to experimental studies of sputter deposition.

I. INTRODUCTION

In deposition or etching processes, shadowing is often a factor in the evolution of the interface. In such processes, uncollimated particles are incident on a substrate and, upon contact with the substrate surface, either etch the surface or are deposited on it. Shadowing implies that a given point on the surface can receive fewer particles than other points, because nearby surface features block some of the incoming particles. This is illustrated in Fig. 1. This sort of process is believed to be important in sputter deposition of thin films.

There have been several experimental studies of roughening in sputter deposited films.[1–6]. As can be seen in Table I, a wide range of scaling exponents has been observed, and the observed exponents seem to depend on the experimental conditions as well as the deposition species. For example, You *et al.* obtained a value of 0.40 for the growth exponent β and a value of 0.40 for the roughness exponent α for sputter deposition of gold at 300 K,[1] while Wang *et al.* found that $\beta=0.42$ and $\alpha=0.89\pm0.05$ for sputter deposition of molybdenum at room temperature.[2] Lee, Cahill, and Greene studied sputter deposition of silicon onto singular and miscut silicon substrates at 300 °C and found $\beta=0.7\pm0.05$ and $\alpha=0.80\pm0.05$ for the miscut substrates and $\beta=0.6\pm0.05$ and $\alpha=0.85\pm0.05$ for the singular substrates.[3] Le Bellac, Niklasson, and Granqvist studied the scaling of chromium films prepared by oblique sputter deposition at 300–330 K and found $\beta=0.98\pm0.1$ and $\alpha\approx1$.[4] They also found that the average column diameter ζ obeyed $\zeta\propto t^{0.98\pm0.1}$.[4] For sputter deposition of copper at 450 K, Eisenmenger-Sittner *et al.* found that $\beta=1/3$,[5] while Karr *et al.* found, for sputter deposition of TiN at 750 °C, that $\beta=0.25\pm0.07$, and that the average mound separation was proportional to $t^{0.25\pm0.07}$.[6]

Both numerical calculations and Monte Carlo simulations of shadowing have been carried out, but so far, most of the theoretical studies have been performed in $1+1$ dimensions.[7–13] This is due to the extreme difficulty of studying nonlocal models, like shadowing, in $2+1$ dimensions. Yao and Guo proposed a continuum equation for shadowing growth in $2+1$ dimensions.[14]

$$\frac{\partial h}{\partial t}=\nu\nabla^2 h+R\Omega(\mathbf{r},\{h\})+\eta(\mathbf{r},t). \tag{1}$$

The first term on the right-hand side of this equation is a condensation-evaporation term. The Ω in Eq. (1) is the exposure solid angle. The last term is a noise term. The numerical calculations, on a 96×96 lattice, of Yao and Guo show that the interface width w increases linearly with time and that the column width ζ grows as $\zeta\propto t^{0.33\pm0.02}$.[14] However, their model does not include the possibility of growth normal to the local surface that occurs experimentally during sputter deposition.

In this paper, we examine a $(2+1)$-dimensional continuum model of shadowing with surface normal growth and present a detailed Monte Carlo study of a discrete $(2+1)$-dimensional shadowing model, with inherent lateral growth, similar to the $(1+1)$-dimensional model of Roland and Guo.[11] Our results are compared to published experimental findings. We also examine the dynamic scaling behavior of etching in the presence of shadowing.

II. CONTINUUM MODEL OF SHADOWING

Here we use a continuum model in which the surface is described by a height function $h(\mathbf{r},t)$, where t refers to time and $\mathbf{r}=(x,y)$. Further, we impose the periodic condition that $h(x+N,y+N,t)=h(x,y,t)$ for a system size of $N\times N$. Shadowing growth and etching can be considered a special case of the nonlocal model that we recently studied.[15]

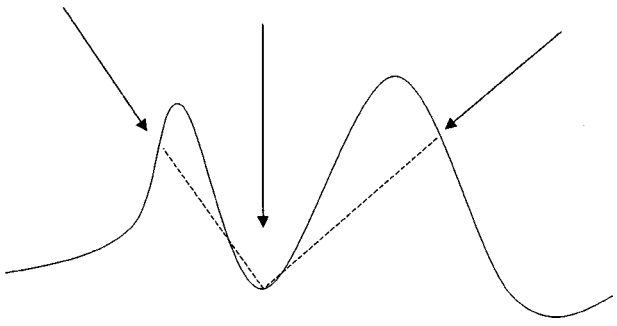

FIG. 1. Illustration of the shadowing effect. The valley receives fewer incoming particles than the peaks, because incoming particles are blocked by the peaks.

TABLE I. The observed exponents for several sputter deposition experiments. For comparison, theoretical shadowing results are shown below the double line.

System/model	Film structure/model type	Temperature/number of dimensions	α	β	p	Reference
Au on Si (111)		220 K	0.42	0.42		1
		300 K	0.40	0.40		
Mo on Si (111)		Room temperature	0.89 ± 0.05	0.42		2
Si on Si (001):						3
Singular	Epitaxial	300 °C	0.85 ± 0.05	0.6 ± 0.05		
Miscut	Epitaxial	300 °C	0.80 ± 0.05	0.7 ± 0.05		
Cr (oblique incidence)		300–330 K	1	0.98 ± 0.1	0.98 ± 0.1	4
Cu on oxidized Si (100)		450 K		1/3		5
TiN (001) on MgO (001)	Epitaxial	750 °C		0.25 ± 0.07	0.25 ± 0.07	6
Shadowing growth (without lateral growth)	Continuum	$1+1$		1	0.7	12
Shadowing growth (with lateral growth)	Continuum	$1+1$		1	1	12
Shadowing growth	Monte Carlo	$1+1$			$0.55-0.58$	11
Shadowing growth	Continuum	$2+1$		1	0.33 ± 0.02	14
Shadowing growth	Continuum	$2+1$		1		This work
Shadowing etching	Continuum	$2+1$		0		This work
Shadowing growth	Monte Carlo	$2+1$		1	0.93 ± 0.1	This work
Shadowing etching	Monte Carlo	$2+1$	0	0	0	This work

$$\frac{\partial h}{\partial t}=\nu\nabla^2 h-\kappa\nabla^4 h\mp\sqrt{1+(\nabla h)^2}\times[s_0F_0(\mathbf{r},t)+s_1F_1(\mathbf{r},t)+\cdots]+\eta. \quad (2)$$

The first two terms on the right-hand side of this equation are the familiar smoothing mechanisms of condensation and evaporation and surface diffusion, respectively. The last term is the noise term, and the third term is a nonlinear term corresponding to flux reemission. The factor $\mp\sqrt{1+(\nabla h)^2}$ is present because the growth and etching are normal to the local surface. Here, the ''+'' sign corresponds to a growth process and the ''−'' sign refers to an etching process. In this model, particles are labeled based on the number of times that they have collided with the surface. For example, an nth-order particle is a particle that has collided n times with the surface. If an nth-order particle collides with the surface, there is a probability s_n of the particle sticking. If the particle sticks, it will either deposit on the surface or etch the surface, depending on whether the process is deposition or etching. If the particle does not stick, then it will be reemitted and go elsewhere. The flux of nth-order particles at a position $\mathbf{r}$ on the surface is $F_n(\mathbf{r},t)$ and can be found by the equation[15]

$$F_{n+1}(\mathbf{r},t)=(1-s_n)\int Z(\mathbf{r},\mathbf{r}',t)F_n(\mathbf{r}',t)\times\frac{(\hat{\mathbf{n}}_{\mathbf{rr}'}\cdot\hat{\mathbf{n}})P(\hat{\mathbf{n}}_{\mathbf{r}'\mathbf{r}},\hat{\mathbf{n}}')}{(\mathbf{r}-\mathbf{r}')^2+(h-h')^2}dA', \quad (3)$$

where $\hat{\mathbf{n}}$ is the unit normal, at position $\mathbf{r}$, pointing out of the surface, $\hat{\mathbf{n}}'$ is the unit normal at position $\mathbf{r}'$, $\hat{\mathbf{n}}_{\mathbf{rr}'}$ is a unit vector pointing from $\mathbf{r}$ to $\mathbf{r}'$, and $\hat{\mathbf{n}}_{\mathbf{r}'\mathbf{r}}$ is a unit vector pointing from $\mathbf{r}'$ to $\mathbf{r}$. Here $P(\hat{\mathbf{n}}_{\mathbf{r}'\mathbf{r}},\hat{\mathbf{n}}')$ is the probability per solid angle that a reemitted particle will go off in the direction of

$\hat{\mathbf{n}}_{\mathbf{rr}'}$. Also, $Z(\mathbf{r},\mathbf{r}',t)$ is equal to 1 unless there is no line of sight between the surface elements at $\mathbf{r}$ and $\mathbf{r}'$ or $(\hat{\mathbf{n}}_{\mathbf{rr}'}\cdot\mathbf{n})$ is negative, in which case Z is zero.

Equation (2) can be used to describe many transport limited growth-etching processes. For example, we have recently proposed that plasma etch-front roughening corresponds to first-order reemission: $s_0\approx 0$ and $s_1=1$.[15] The case of shadowing corresponds to zeroth-order reemission: $s_0=1$ and $s_n\approx 0$ for $n>0$. In this case, Eq. (2) becomes

$$\frac{\partial h}{\partial t}=\nu\nabla^2 h-\kappa\nabla^4 h\mp s_0 F_0(\mathbf{r},t)\sqrt{1+(\nabla h)^2}+\eta, \tag{4}$$

with

$$F_0(\mathbf{r},t)=\int\int \mathbf{J}(\theta,\phi)\cdot\hat{\mathbf{n}}(\mathbf{r})\,d\Omega$$
$$=\int_0^{2\pi}\int_0^{\theta_{\max}(\phi)}\mathbf{J}(\theta,\phi)\cdot\hat{\mathbf{n}}(\mathbf{r})(\sin\theta)\,d\theta\,d\phi, \tag{5}$$

where θ is the local polar angle and ϕ is the local azimuthal angle. Also, $\mathbf{J}(\theta,\phi)=R(\theta,\phi)[\sin\theta(\hat{\imath}\cos\phi+\hat{\jmath}\sin\phi)+\hat{k}\cos\theta]$, where $R(\theta,\phi)$ is the distribution of the incoming flux. We can see that F_0 contains information about the shadowing effect of the surrounding surface features, as well as the nature of the incoming flux. Unlike Eq. (1), our model includes growth normal to the local surface. Solutions to Eq. (2) are found by numerical integration.

III. DISCRETE MODEL OF SHADOWING

For the discrete model, the surface is again described by a height function $h(\mathbf{r},t)$, where t refers to time and $\mathbf{r}=(x,y)$. However, because the model we use is discrete, x, y, and h can take on only integer values. Furthermore, because h is single valued, this model does not allow for the possibility of overhangs. Finally, we again impose the periodic condition that $h(x+N,y+N,t)=h(x,y,t)$ for a system size of $N\times N$.

A position in the x-y plane is chosen at random. This is used as the initial in-plane position for a particle that will etch or deposit on the surface. The initial height of the particle is taken to be $\max(h)+1$. A direction for the particle is then chosen, and the particle proceeds in this direction until it hits the surface. The distribution of directions is given by

$$\frac{dP}{d\Omega}=\frac{\cos\theta}{\pi}. \tag{6}$$

Upon striking the surface, the particle sticks at the point of impact. However, if the particle hits the side of a column, it slides straight down until it hits the surface again, as shown in Fig. 2(a). This is exactly what happens in the model of Roland and Guo.[11] In this way, overhangs are prevented. Also, growth normal to the local surface is implicitly accounted for in this model. For etching, the simulation proceeds as for growth except that, when a particle hits a column, the height of the surface at the point of impact is decreased by 1. This is shown in Fig. 2(b); an incident particle (1) impacts the surface and etches the surface at the point of impact (2). All particles (3) above the point of impact move down one space.

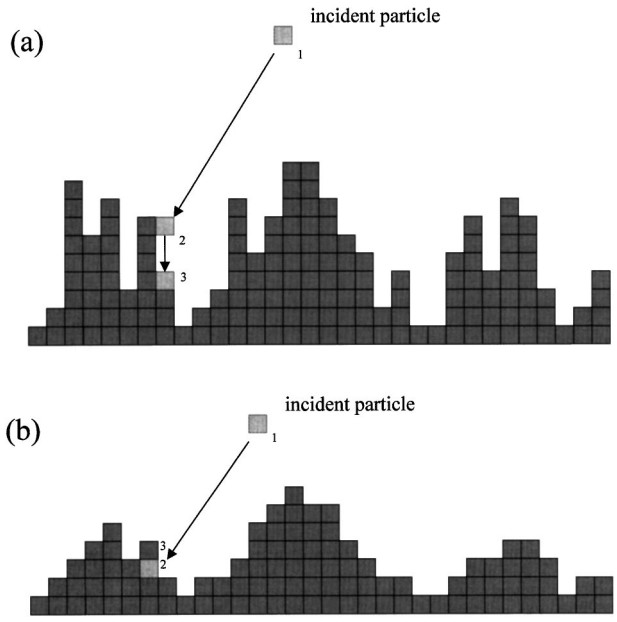

FIG. 2. Illustration of the Monte Carlo simulations for (a) growth and (b) etching.

IV. NUMERICAL CALCULATIONS AND MONTE CARLO SIMULATIONS

For both the numerical calculations and Monte Carlo simulations, it is possible to extract quantitative information about the growth or etching process from the generated surfaces. A useful quantity is the interface width w, defined by

$$w^2=\langle[h(\mathbf{r},t)-\overline{h}(t)]^2\rangle, \tag{7}$$

where $\overline{h}(t)$ is the average height of the surface at time t and $\langle\cdots\rangle$ denotes an average over the entire surface. We assume that

$$w\propto t^{\beta}, \tag{8}$$

where β is called the growth exponent. We define the autocorrelation function as

$$C(r)=\langle[h(\mathbf{r}'+\mathbf{r})-\overline{h}(t)][h(\mathbf{r}')-\overline{h}(t)]\rangle, \tag{9}$$

where $r=|\mathbf{r}|$. For $r=0$, $C(r)=w^2$. Note that we have assumed that the surfaces are isotropic. From the autocorrelation function, one can determine the correlation length ξ, defined by

$$C(\xi)=w^2/e. \tag{10}$$

We assume that

$$\xi\propto(t-t_0)^{1/z}, \tag{11}$$

where z is called the dynamic exponent and t_0 is the crossover time. The height-height correlation function $H(r)$ is defined by

$$H(r)=\langle[h(\mathbf{r}+\mathbf{r}',t)-h(\mathbf{r}',t)]^2\rangle, \tag{12}$$

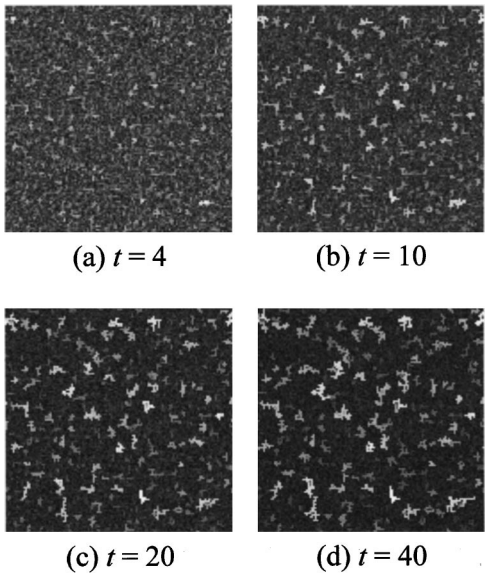

FIG. 3. Surface images for the 128×128 numerical calculation of shadowing growth at (a) $t=4$, (b) $t=10$, (c) $t=20$, and (d) $t=40$. Light areas indicate high h, while dark areas indicate low h.

and we can get the roughness exponent α from the relation

$$H(r)\propto r^{2\alpha} \quad \text{for } r\ll\xi. \tag{13}$$

We can also analyze the power spectrum density, defined by

$$P(\mathbf{k},t)=\left|\frac{1}{2\pi}\int [h(\mathbf{r},t)-h(t)]e^{i\mathbf{k}\cdot\mathbf{r}}d\mathbf{r}\right|^2. \tag{14}$$

It is then useful to look at the location k_0 of the maximum in the circular average of the power spectrum. From this, we can find the average column width $\zeta=2\pi/k_0$. We assume that the average column width behaves as

$$\zeta\propto(t-t_0)^p. \tag{15}$$

A. Shadowing growth

The numerical calculations of the continuum equation were performed on a 128×128 lattice, and we set ν and κ equal to zero. In Fig. 3 we show the surface morphology for the growth model at various times. The morphology consists of tall columns, and the distance between neighboring columns (of similar height) is large compared to the column size. To make this point more clear, we show, in Fig. 4, a cross section of one of the surfaces. In Fig. 5(a), we plot the interface width w versus time t. We see a clear linear dependence of w on t, just as observed by Yao and Guo in their $(2+1)$-dimensional numerical calculations.[14] Due to the small system size, we could not get reliable values for the dynamic exponent from the numerical calculations.

Because the Monte Carlo simulation is more efficient than the numerical calculation, 1024×1024 simulations were run. The surface morphology, at various times, for the growth simulation, is shown in Fig. 6. In Fig. 7 we show the cross sections of the surface morphology for various growth times. The cross-sectional morphology consists of columns that grow taller and wider with increasing growth time. This is the same type of morphology observed by Roland and Guo

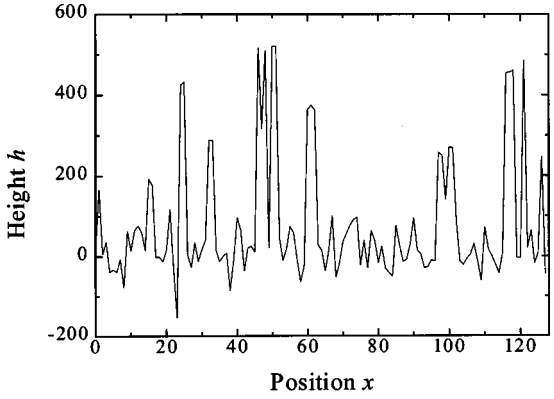

FIG. 4. Cross section of the surface of the 128×128 numerical calculation at $t=40$. The surface appears to contain tall, widely separated columns.

in their $(1+1)$-dimensional simulations.[11] Note, however, that this morphology differs from the morphology seen in the continuum model; in the continuum model, the columns were spread farther apart (compared to the column size) than in the discrete model. The discrepancy is probably due to the fact that, in the discrete model, particles hitting the side of a column were allowed to slide down the column. In Fig. 5(b), the interface width w is plotted as a function of growth time t. There is a clear linear dependence of the interface width on time, which implies that $\beta=1$. In Fig. 8, we plot the correlation length ξ and the column width ζ as a function of growth time t, respectively. The correlation length appears to have a linear dependence on time, but does not intercept the origin. Fitting the function $A(t-t_0)^{1/z}$ to the data gave $1/z=0.93\pm0.1$. The average column width shows similar time dependence, but it is much less clear whether this dependence is linear or not.

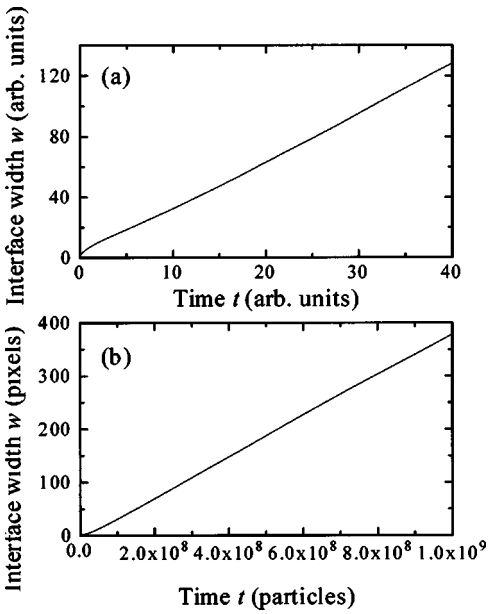

FIG. 5. (a) Interface width vs time for the 128×128 numerical calculation of shadowing growth. The clear linear dependence of w on t implies that $\beta=1$. (b) Interface width vs time for the 1024×1024 shadowing growth simulation. The clear linear dependence of w on t implies that $\beta=1$.

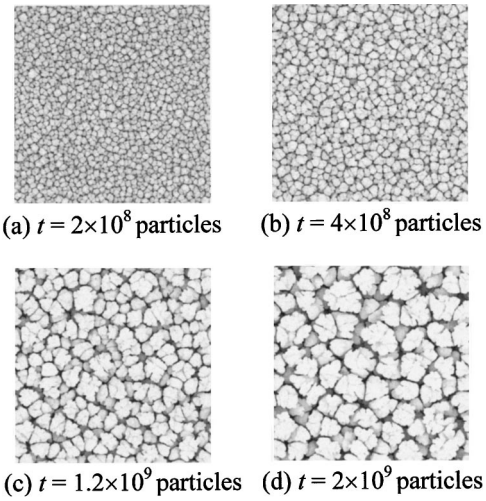

FIG. 6. Surface images for the 1024×1024 Monte Carlo simulation of shadowing growth at (a) $t=2\times10^8$ particles, (b) $t=4\times10^8$ particles, (c) $t=1.2\times10^9$ particles, and (d) $t=2\times10^9$ particles. Light areas indicate high h, while dark areas indicate low h.

The results that we obtain for the interface width are the same as the results obtained by Yao and Guo for the $(2+1)$-dimensional continuum model.[14] The linear increase of w is also seen in the columnar phase of the $(1+1)$-dimensional discrete model of Yao, Roland, and Guo.[12] It seems clear that shadowing growth leads to a linear dependence of the interface width on time, but the situation for ξ and ζ is more complicated. Our values for ζ are less reliable than our values for ξ, but if we assume that surfaces at different times are statistically identical except for a scale change, then the exponent p should be equal to $1/z$. We illustrate this point in Fig. 9 by showing the circularly averaged power spectra of the surfaces at different times, resealed by a factor of $t^{2\beta}(t-t_0)^{2/z}$ vertically and by a factor of $(t-t_0)^{-1/z}$ horizontally. The fact that the power spectra overlap indicates that, while the surface features get bigger both vertically and horizontally, they do not otherwise change very much. Yao and Guo found that $p=0.33\pm0.02$ in $2+1$ dimensions.[14] This differs significantly from our value of $1/z=0.93\pm0.1$, but Yao and Guo did not take lateral growth into account in their calculations. While lateral growth does not seem to affect the behavior of the interface width, it is reasonable to suspect that it would have a significant influence on the behavior of both the correlation length and the average column width. Yao, Roland, and Guo found that $p=0.7$ in $1+1$ dimensions and that $p=1$ in $1+1$ dimensions with a lateral growth term.[12]

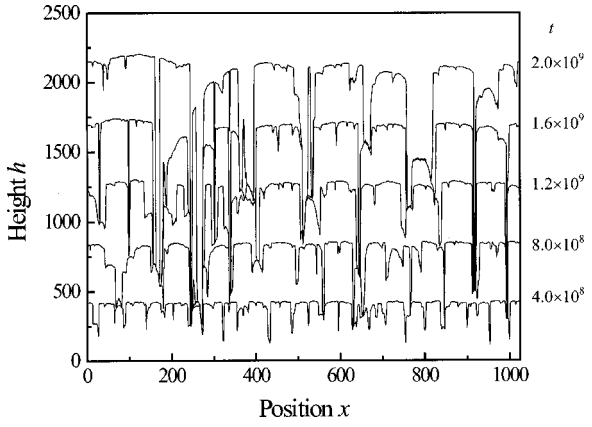

FIG. 7. Cross sections of the surface of the 1024×1024 shadowing growth simulation for various growth times: $t=4.0\times10^8$, $t=8.0\times10^8$, $t=1.2\times10^9$, $t=1.6\times10^9$, and $t=2.0\times10^9$. The surfaces appear to consist of tall columns.

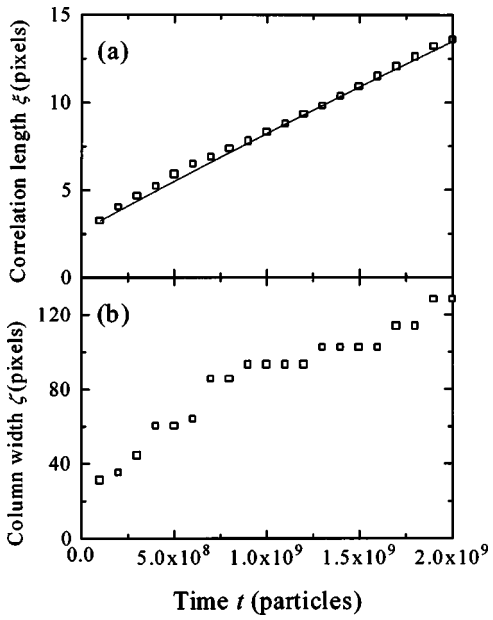

FIG. 8. (a) Plot of correlation length ξ vs time for the 1024×1024 shadowing growth simulation. The solid line indicates the best fit of the function $A(t-t_0)^{1/z}$, which gives $A=2.45\times10^{-8}$, $t_0=-4.25\times10^8$, and $1/z=0.93\pm0.1$. (b) Plot of average column width ζ vs time for the 1024×1024 shadowing growth simulation.

Our $(2+1)$-dimensional Monte Carlo results are quite different from the $(1+1)$-dimensional Monte Carlo results of Roland and Guo, in which they found that p ranges between 0.55 and 0.58, depending on the width of the angular distribution of the incoming flux (the maximum angle of the flux $\theta_{\max}$ was varied from 30° to 70°).[11] This supports the

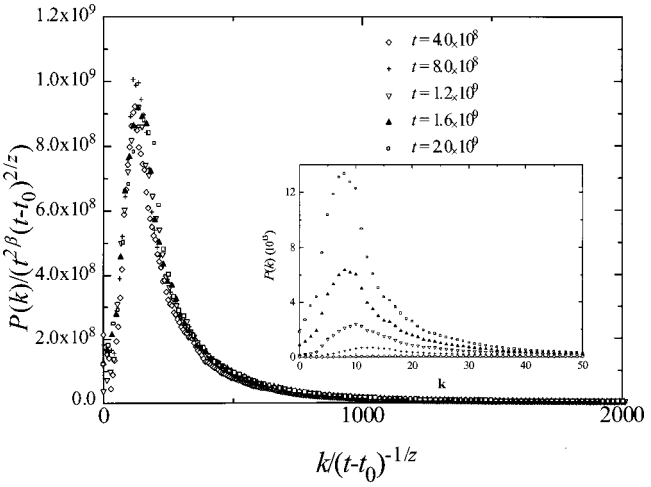

FIG. 9. Rescaled circular averaged power spectra for the shadowing growth simulation for $t=4.0\times10^8$, $t=8.0\times10^8$, $t=1.2\times10^9$, $t=1.6\times10^9$, and $t=2.0\times10^9$. The inset shows the unscaled data.

view that the scaling properties are not sensitive to the angular distribution of the incoming flux. In our simulations, we did not limit the angular distribution of the incoming flux (corresponding to $\theta_{max}=90°$). Our value for $1/z$ ($=0.93 \pm 0.1$) is larger than the value of p (between 0.55 and 0.58) obtained by Roland and Guo. The discrepancy could be due to the difference in dimensionality ($2+1$ dimensions instead of $1+1$ dimensions), or it could be due to the presence of other factors, such as surface diffusion or condensation and evaporation, in the simulations of Roland and Guo.

Our results for shadowing growth agree quite well with the experimental results of Bellac, Niklasson, and Granqvist.[4] However, in their experiment, the deposition was at an oblique angle, while in our simulations, the flux came from all directions. The growth exponents found by Lee, Cahill, and Greene, while significantly lower than the growth exponent found in our simulations, are significantly larger than 1/2.[3] This means that there must be a roughening mechanism present besides noise. Smoothing effects, such as surface diffusion, could only lower the exponent, but shadowing gives a growth exponent much greater than 1/2. Hence shadowing combined with a smoothing mechanism could result in a growth exponent greater than 1/2, but less than 1.

The growth exponents found by You *et al.*[1] and Wang *et al.*[2] differ greatly from our value, but, again, smoothing effects could be present. Also, other factors, such as the angular spread of the flux, will affect the exponents. The experiment of Eisenmenger-Sittner *et al.*[5] and the experiment of Karr *et al.*[6] give the smallest exponents. In those experiments, however, surface diffusion is probably the dominant mechanism.

It is clear that a large discrepancy exists between the sputter deposition experiments and our model. However, for most cases, other processes, such as surface diffusion, are also present. This can lead to a substantial lowering of the observed exponents, thus explaining the discrepancy. One might be tempted to assert that the shadowing effect should always win out over linear effects such as surface diffusion. While this might be true, the crossover time from diffusive to shadowing behavior can, for sufficiently high surface diffusion, be large enough to prevent shadowing behavior from being observed. Further, it is far from clear how other processes interact with a shadowing term. Another possibility is that, in some of the experiments, the film might be polycrystalline. For polycrystalline films, the grain formation process will affect the growth. For such a case, it is reasonable to expect that the scaling exponents would differ from the values predicted by a pure shadowing model.

B. Shadowing etching

The basic idea of the shadowing effect in sputtering growth is that the crest of the surface will receive more deposited atoms than the valley of the surface because the receiving solid angle at the crest is larger than that in the valley. Therefore the growth rate at the peak is faster than at the valley, which causes the growth instability. However, if one applies this model to an etching process, suggesting that peaks have a faster etching rate than valleys, one would expect stable growth with a growth exponent $\beta<0.5$. That is, shadowing is a smoothing mechanism for the case of etching.

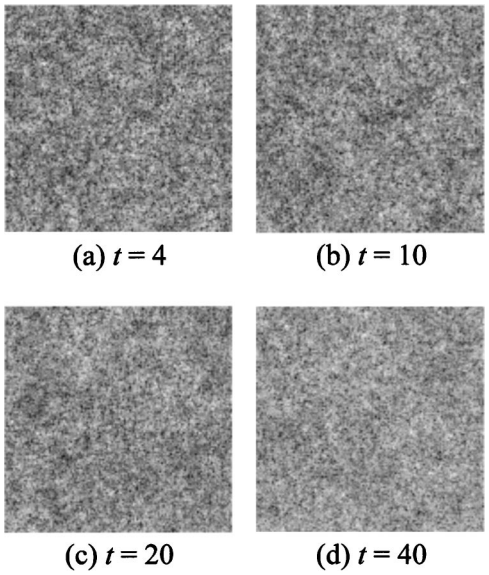

FIG. 10. Surface images for the 128×128 numerical calculation of shadowing etching at (a) $t=4$, (b) $t=10$, (c) $t=20$, and (d) $t=40$. Light areas indicate high h, while dark areas indicate low h.

For the numerical calculations of etching, a 128×128 lattice was again used. The morphology for the numerical calculation is shown in Fig. 10. We can see that the surface changes very little over the range of times covered in the calculation. In Fig. 11(a), we plot the interface width w versus time t in semilogarithmic scale. From the plot, we can see that w increases initially because of the noise, but eventually flattens out. This implies that $\beta=0$.

The surface morphology for the Monte Carlo etching simulation is shown in Fig. 12. The morphology, in this case,

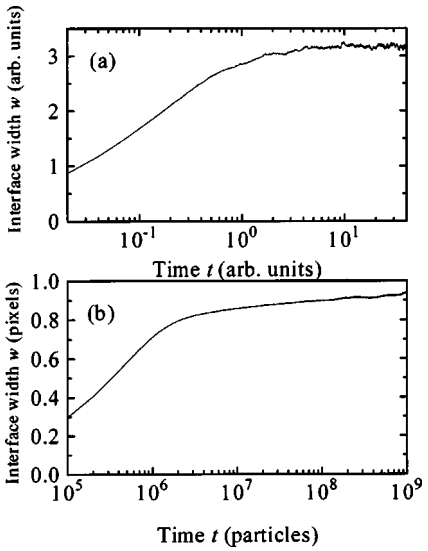

FIG. 11. (a) Semilogarithmic plot of interface width vs time for the 128×128 numerical calculation of shadowing etching. The fact that w saturates, for later times, indicates that $\beta=0$. (b) Semilogarithmic plot of interface width vs time for the 1024×1024 shadowing etching simulation. The linear dependence of w on t, for later times, indicates that $\beta=0$.

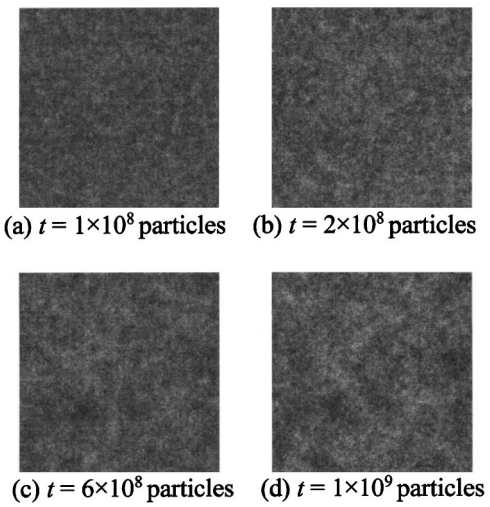

FIG. 12. Surface images for the 1024×1024 Monte Carlo simulation of shadowing etching at (a) $t=1\times10^8$ particles, (b) $t=2\times10^8$ particles, (c) $t=6\times10^8$ particles, and (d) $t=1\times10^9$ particles. Light areas indicate high h, while dark areas indicate low h.

is rather unremarkable. For the etching process, the only roughening mechanism present is noise. Initially, the interface roughens due to the noise. However, the shadowing effect eventually becomes important, and the surface changes very little after that point. In Fig. 11(b), we plot, in semilogarithmic scale, the interface width versus time. After the initial noise regime, the interface width increases only slightly, and we see a linear dependence of w on $\log(t)$. This implies that $\beta=0$. In Fig. 13, we plot, in semilogarithmic scale, the height-height correlation functions for different times. There are two interesting features of this plot. First, $H(r)$ is linear in $\log(r)$ for $r\ll\xi$. This implies that $\alpha=0$. Second, all later height-height correlation functions ($t\geq2.0\times10^8$) almost overlap the last one shown. This confirms the fact that $\beta=0$ and also indicates that $1/z=0$. These exponents have not been observed experimentally. However, in cases where shadowing etching might be present, such as plasma etching, the first order term in Eq. (2) can also play an important role.[15]

It is a common belief that etching is the reverse process of growth. One can define an etching exponent β_e instead of the growth exponent β_g if the same mechanism works for both the etching and growth processes. Recently, we have discussed that all the well-known local growth-etching models give $\beta_e=\beta_g$, while for nonlocal growth-etching models, $\beta_e\neq\beta_g$.[15] Our simulations have shown that for the shadowing effect, growth gives $\beta_g=1$, while etching gives $\beta_e=0$. This is consistent with the nonlocal nature of the shadowing model.

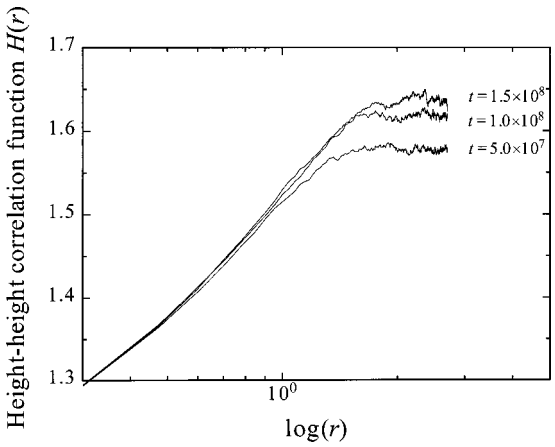

FIG. 13. Height-height correlation functions for the shadowing etching simulation for $t=5.0\times10^7$, $t=1.0\times10^8$, and $t=1.5\times10^8$. For later times, the height-height correlation functions overlap the $t=1.5\times10^8$ height-height correlation function.

V. CONCLUSION

We have presented the results of $(2+1)$-dimensional numerical calculations and Monte Carlo simulations of shadowing growth and etching. The numerical calculations and Monte Carlo simulations of etching produce rough surfaces that roughen with a growth exponent close to zero. Both the Monte Carlo growth simulations and the numerical growth calculations produce surfaces that consist of tall columns and roughen with an exponent of unity, in agreement with $(1+1)$-dimensional Monte Carlo simulations of shadowing growth and $(1+1)$- and $(2+1)$-dimensional numerical solutions of continuum shadowing models. The surface features coarsen laterally with an exponent close to unity, in contrast to other studies of shadowing growth that predict a smaller exponent. However, differences in dimensionality, or other more subtle differences in models such as the inclusion of lateral growth in our model, can account for this discrepancy. The shadowing growth results do not appear to agree with recent sputter deposition experiments. This is probably due to the presence of other factors besides shadowing in the experiments. It is also possible that, in some of the experiments, the shadowing effect is weakened. Thus it is clear that sputter deposition is not completely described by the shadowing effect. A more complete understanding of the role of shadowing in sputter deposition could be accomplished by varying the deposition parameters in order to find the conditions under which shadowing becomes dominant.

ACKNOWLEDGMENT

This work was supported by the NSF.

[1] H. You, R. P. Chiarello, H. K. Kim, and K. G. Vandervoort, Phys. Rev. Lett. **70**, 2900 (1993).

[2] Jun Wang, Gang Li, Ping Yang, Mingqi Cui, Xiaoming Jiang, Bing Dong, and Hong Liu, Europhys. Lett. **42**, 283 (1998).

[3] N.-E. Lee, David G. Cahill, and J. E. Greene, Phys. Rev. B **53**, 7876 (1996).

[4] D. Le Bellac, G. A. Niklasson, and C. G. Granqvist, Europhys. Lett. **32**, 155 (1995).

[5] C. Eisenmenger-Sittner, H. Bangert, A. Bergauer, and W. Bauer, in *Evolution of Thin-Film and Surface Strucutre and Morphology*, edited by B. G. Demczyk *et al.*, MRS Symposia Proceedings No. 355 (Materials Research Society, Pittsburgh, 1995), p. 395.

[6] B. W. Karr, I. Petrov, P. Desjardins, D. G. Cahill, and J. E. Greene, Surf. Coat. Technol. **94**, 403 (1997).

[7] R. P. U. Karunasiri, R. Bruinsma, and Joseph Rudnick, Phys.

Rev. Lett. **62**, 788 (1989).
[8] R. P. U. Karunasiri, R. Bruinsma, and Joseph Rudnick, in *Proceedings of the Second Woodward Conference*, edited by Lui Lam and C. Hedley Moris (Springer-Verlag, New York, 1990), p. 253.
[9] G. S. Bales and A. Zangwill, Phys. Rev. Lett. **63**, 692 (1989).
[10] G. S. Bales and A. Zangwill, J. Vac. Sci. Technol. A **9**, 145 (1991).
[11] Christopher Roland and Hong Guo, Phys. Rev. Lett. **66**, 2104 (1991).
[12] Jian Hua Yao, Christopher Roland, and Hong Guo, Phys. Rev. A **45**, 3903 (1992).
[13] Joachim Krug and Paul Meakin, Phys. Rev. E **47**, R17 (1993).
[14] Jian Hua Yao and Hong Guo, Phys. Rev. E **47**, 1007 (1993).
[15] Jason T. Drotar, Y.-P. Zhao, T.-M. Lu, and G.-C. Wang, Phys. Rev. B **61**, 3012 (2000).